DELAMINATION DURABILITY OF COMPOSITE MATERIALS FOR ROTORCRAFT

T.Kevin O'Brien

Aerostructures Directorate

U.S. Army Research and Technology Activity (AVSCOM)

NASA Langley Research Center

Hampton, Virginia

Delamination is the most commonly observed failure mode in composite rotorcraft dynamic components. Although delamination may not cause immediate failure of the composite part, it often precipitates component repair or replacement, which inhibits fleet readiness, and results in increased life cycle costs. In this paper, a fracture mechanics approach for analyzing, characterizing, and designing against delamination will be outlined. Examples of delamination problems will be illustrated where the strain energy release rate associated with delamination growth has been found to be a useful generic parameter, independent of thickness, layup, and delamination source, for characterizing delamination failure. Several analysis techniques for calculating strain energy release rates for delaminations from a variety of sources will be outlined. Current efforts to develop ASTM standard test methods for measuring interlaminar fracture toughness and developing delamination failure criteria will be reviewed. A technique for quantifying delamination durability due to cyclic

loading will be presented. The use of this technique for predicting fatigue life of composite laminates and developing a fatigue design philosophy for composite structural components will be reviewed.

FRACTURE MECHANICS ANALYSIS OF DELAMINATION

Potential delamination sites exist in composite structures wherever a discontinuity exists in the load path (ref. 1). These discontinuities give rise to interlaminar stresses even when the remote loading is in-plane. Discontinuities may occur at (1) a straight edge with a stress-free boundary (often called a "free-edge"), (2) a curved stress-free boundary, such as the edge of a drilled hole, (3) a drop-off of the interior plies of a laminate to taper thickness, (4) a bonded or co-cured joint, and (5) a bolted joint (fig. 1). Of these cases, the free-edge delamination problem has been studied most extensively, and illustrates the benefits of fracture mechanics for characterizing delamination behavior.

Army and NASA investigators have analysed the strain energy release rate, G, associated with edge delamination growth (refs. 2-6). From finite element analyses they have found that once the delamination is modeled beyond a few ply thicknesses from the straight edge, G reaches a constant plateau given by the equation shown in figure 2. This equation, derived from a rule of mixtures and laminated plate theory, shows that G is independent of delamination size and depends only on the remote strain, ε, the laminate thickness, t, and two modulus terms, E_{LAM} and E^{*}, that correspond to the laminate modulus before and after delamination. In reference 2, the critical strain, ε_c, measured at the onset of

delamination at the -30/90 interfaces of eleven-ply $(\pm30/\pm30/90/90)_s$ laminates was substituted into the edge delamination equation in fig. 2 to determine a critical G_c for Thornel 300/ Narmco 5208 graphite epoxy composites. This G_c was then used to predict the onset strains for edge delamination in the 0/90 interfaces of $(45_n/-45_n/0_n/90_n)_s$ laminates of the same material, where n=1,2,3 corresponds to an 8-, 16-, and 24-ply laminate. Figure 3 shows that the predictions agreed well with experimental data, and captured the trend of decreasing delamination onset strain with increasing thickness. An analysis based on the critical values of the interlaminar stresses at the straight edge would not account for this thickness dependence because the interlaminar stresses at the straight edge are independent of thickness (ref. 7).

Finite Element Analysis

Because a delamination is constrained to grow between individual plies, both interlaminar tension and shear stresses are commonly present at the delamination front. Therefore, delamination is often a mixed-mode fracture process. A boundary value problem must be formulated and solved to determine the strain energy release rate components at the crack tip: G_I due to interlaminar tension, G_{II} due to sliding shear, and G_{III} due to scissoring shear. A virtual crack extension technique was used in combination with a quasi-three dimensional finite element analysis to calculate the various G components (refs. 2-6). Figure 4 shows the results of such an analysis for delaminations between the 90-deg and neighboring ply in a family of three quasi-isotropic laminates. The 90-deg plies were in the center of each layup, but the 45,-45, and 0-deg plies were permutated to yield three unique stacking sequences. As noted earlier, the total G rises to a constant plateau when the delamination progresses beyond a

few ply thicknesses from the edge. The total G values calculated by the rule of mixtures and by summing the G components from the finite element analysis were nearly identical for all three layups. However, the mixture of the G components was different for each layup. For example, figure 4 shows that the G_I components for the various layups have values ranging from nearly 90% of the total G to less than 30% of the total G. The G_{III} component calculated for each layup was negligible. Hence the difference in the G_I component and total G for each case was the G_{II} contribution. Furthermore, like the total G, the G components are independent of delamination size. As illustrated in a later section, tests conducted on three similar layups, where the ±45-deg plies where changed to ±35-deg based on a parametric study conducted in ref. 4 to minimize the ε_c required to measure a given G_c, were used to develop mixed-mode interlaminar fracture criteria for composite materials (ref. 5).

Residual Thermal Stress Contributions to G

Composite laminates are manufactured, or cured, under temperature and pressure and then cooled to room temperature for testing. During cooling from the cure temperature, the plies of the laminate that are oriented at different angles would like to contract differently, but they are forced to contract equally. This constraint leads to the development of residual thermal stresses in the individual plies. When a composite delaminates, part of the strain energy released may be attributed to these residual thermal stresses. A previously developed analysis for the strain energy release rate associated with edge delamination in composite laminates was modified to include the contribution of residual thermal stresses (ref. 6). This analysis was performed for several materials to determine the influence of the residual thermal stresses on

delamination formation and growth. Figure 5 shows the strain energy release rate, G^{M+T}, for edge delamination in a $(25/-25/90)_s$ laminate due to a combination of mechanical (M) and thermal (T) loads, as a function of the thermal gradient, ΔT, between the cure or consolidation temperature and room temperature. The value of G calculated for mechanical loading only is shown on the ordinate where $\Delta T=0$. The other value indicated by a symbol corresponds to G where both the mechanical load and the appropriate ΔT for the material were included in the analysis. For a graphite fiber composite with a brittle epoxy matrix, delaminations occur at mechanical strains around 0.004, and the contribution of residual thermal stresses to G is small. However, for a high modulus graphite fiber composite with a brittle bismaleimide (BMI) matrix that is cured at a higher temperature than epoxy, nearly one half of the strain energy released at a strain of 0.004 is attributed to the residual thermal stresses. Composite laminates made with thermoplastic matrices are typically much tougher, delaminating at mechanical strains of nearly 0.01. However, thermoplastic matrix composites are manufactured at extremely high temperatures, resulting in a significant residual thermal stress contribution to the strain energy release rate for delamination (ref. 8). Hence, the influence of residual thermal stresses on delamination is significant for materials manufactured at high temperatures.

DELAMINATION ANALYSIS OF STRUCTURAL DETAILS

Delamination Around an Open Hole

A rotated straight edge technique has been used to determine delamination onset around an open hole in a composite laminate (ref. 9). This technique, which is

illustrated in figure 6, involves analysing each angular position, θ, around the hole boundary as if it was the straight edge of a laminate whose plies were rotated from the original orientation by θ degrees. The rotated layup was assumed to be subjected to a uniaxial strain equal to the circumferential strain at the hole boundary. Using these assumptions the equation for strain energy release rate associated with straight edge delamination may be used as shown in figure 6, where the strain and modulus terms are functions of θ, to generate G distributions around the hole boundary for each unique interface in the laminate. Figure 7 shows a radial plot of a nondimensionalized G parameter in the 45/90 interface of a quasi-isotropic $(45/90/-45/0)_s$ laminate. The position of the maximum G on the hole boundary is located using this technique. Furthermore, finite element analyses may be performed using the techniques described earlier for straight edge delaminations to determine the G_I distribution around the hole boundary, shown by the shaded region in figure 7.

Higher order plate theory analysis of delamination

Previously, a finite element analysis was required to determine the relative contributions of G_I, G_{II}, and G_{III} to the total strain energy release rate for delamination. Although these finite element analyses are useful, they are typically not performed during the design of the structure until the final design stage or until a problem has arisen during qualification testing or in service. Because delamination failures may depend on the ratio of these fracture modes, calculations of G_I, G_{II}, and G_{III} may be needed to accurately anticipate delamination failures. A simple "desk-top" computer analysis for calculating the strain energy release rate, G, components for edge delamination has been

developed by Georgia Tech under an Army/NASA Grant (NAG-1-558). The analysis models the two shearing modes using shear deformation theory to calculate G_{II} and G_{III} directly, then G_I is determined by subtracting the two shear components from the total G. Results from this analysis were compared to finite element results calculated for delamination around an open hole using the rotated straight edge technique. Figure 8 shows results for delamination in the 90/-45 interface of a $(45/90/-45/0)_s$ laminate with a circular hole. As shown in the figure, the higher order plate theory (HPT) yields results that are similar to the finite element (FEM) results; however, the HPT analysis may be performed quickly using a desk top computer. The simple nature of the HPT method makes it suitable for preliminary design analyses which require the evaluation of a large number of configurations, quickly and economically.

Delamination Due to Internal Ply-Drops

Composite rotor hubs, currently being designed and manufactured, are hingeless and bearingless to reduce weight, drag, and the total number of parts. These composite hubs typically have a flapping flexure region where the laminate thickness is reduced by dropping internal plies. Delamination failures are often observed at these ply drops due to the combined centrifugal tension and bending loads applied at the flexure regions of the hub. Although these delaminations may not cause component failure, and therefor yield a desirable benign failure mode, the low delamination durability of current composite materials may result in high repair or replacement costs for the composite hubs. In order to design these composite hubs for delamination durability, analyses are needed that model the delamination failure mode observed. To this end, a simple model was developed for the strain energy release rate associated with delamination growth

from internal ply drops in laminates subjected to tension loads (ref. 10). The delamination was assumed to occur at the first transition from the thin section into the tapered region, labeled point A in figure 9. A simple free body diagram revealed that the maximum interlaminar tensile stress resultant would occur at this point. As shown in figure 9, this local transition region was idealized as a flat laminate with a stiffness discontinuity in the outer "belt" plies and a continuous stiffness in the internal "core" plies. The belt stiffness in the tapered region, E_2, was obtained from a tensor transformation of the belt stiffness in the thin region, E_1, transformed through the taper angle, β. The resulting equation for the strain energy release rate, G, shown in figure 9, is a function of the thicknesses and moduli of the core plies and the belt plies in the tapered region compared to the original thickness, t, and modulus, E_{LAM}, of the thin section of the laminate where the internal plies have been dropped. Furthermore, G was independent of the delamination length, a. Because the belt stiffness in the tapered region is a function of the taper angle, β, G will increase as β increases. Figure 9 shows the increase in G, normalized by the applied tensile load per unit width squared, N_x^2, as the taper angle is increased for a $[0_9/(\pm 45)_2]_s$ glass epoxy laminate. Therefor, the taper angle and ply thicknesses must be considered along with the layup to optimize the rotor hub design for the desired structural performance while minimizing the probability of a delamination failure.

DELAMINATION FAILURE CRITERIA

Interlaminar Fracture Toughness Characterization

Because delamination is the most commonly observed composite failure mode, the need for standard test methods to develop delamination failure criteria has become paramount. To meet this need, a round robin test program has been organized within ASTM committee D30 on High Modulus Fibers and Their Composites to develop standard tests for measuring the interlaminar fracture toughness of composites. Four test methods are being evaluated for their ability to rank materials for improved delamination resistance, to compare toughness measurements between the various tests, and to check the repeatability of measurements between laboratories. The four tests included in the round robin are the double cantilever beam (DCB) test, the edge delamination tension (EDT) test, the cracked lap shear (CLS) test, and the end-notched flexure (ENF) test. These four tests measure critical values of the strain energy release rate, G, for delamination that range from a pure opening mode due to interlaminar tension, G_I, to a pure interlaminar shear mode, G_{II}. The data from these four tests may be used to generate delamination failure criteria for composite materials. As depicted in figure 10, all four test methods will be conducted with three different composite materials with the same AS4 graphite fiber, but with polymer matrices that range from very brittle to very tough. The matrices chosen were (1) Hercules 3501-6, (2) Cyanamid BP 907, and (3) ICI Polyetheretherketone (PEEK). A total of thirty-two laboratories, from five different countries, will be participating in the round robin. Each test will be conducted by at least nine participants. The results of this round robin will be

used to develop ASTM test standards for interlaminar fracture toughness measurement.

Results from edge delamination tension (EDT) tests, pure mode I double cantilever beam (DCB) tests, pure mode II end-notched flexure (ENF) tests, and mixed-mode cracked-lap-shear (CLS) tests have already been used to determine delamination failure criteria for several composite materials (ref. 11). Data are plotted in figure 11, where the G_I component at failure is plotted versus the G_{II} component at failure, for graphite reinforced composite laminates with matrices ranging from very brittle (3501-6, 5208) to very tough (PEEK, F185). In all cases, a linear failure criterion of the form $(G_I/G_{Ic} + G_{II}/G_{IIc}) = 1$ fit the data well. However, for the brittle matrix composites, G_{Ic} is much less than G_{IIc}; whereas for the toughened matrix composites, G_{Ic} is nearly equal to G_{IIc}.

Delamination Durability Under Cyclic Loading

Delamination may occur at cyclic strain levels corresponding to cyclic G levels well below the interlaminar fracture toughness of the composite (ref. 4,8,12,13). Delaminations form at these lower cyclic strains after a certain number of cycles, N. In ref.4, cyclic edge delamination tests were conducted where the G_c values calculated from maximum cyclic strains were plotted as a function of the number of cycles to edge delamination onset (figure 12). These G_c values drop sharply in the first 200,000 cycles until they reach a plateau tantamount to a threshold for delamination onset in fatigue. A finite element analysis of the $(35/-35/0/90)_s$ and $(0/35/-35/90)_s$ laminates tested yielded an identical total G for a given nominal strain, but the G_I

components were very high and low, respectively. As shown in figure 12, the G_c for these two layups measured in static tests (N=1) were different. However, the G_c thresholds under cyclic loading were nearly identical. Hence, the total G does not determine the delamination onset under static loading, but the total G does appear to control the delamination onset in fatigue. Furthermore, a comparison of the relatively tough Hexcel 205 matrix composites to the brittle 5208 matrix composites shows a significant improvement in the static G_c, but the magnitude of this improvement for the G_c threshold in fatigue is much less, as shown in figure 12. A similar trend is shown in figure 13 where the maximum cyclic G_c is plotted as a function of log-cycles to delamination onset for four materials with a wide range of static toughnesses. The matrix materials were (1) Narmco 5208, a 350°F brittle epoxy, (2) Hexcel H205, a 250°F epoxy, (3) Cyanamid HST7, a 350°F epoxy with a tough adhesive interleaf between each ply, and (4) ICI Polyetheretherketone (PEEK), a semicrystalline thermoplastic. When cycles to delamination onset are plotted on a log scale as in figure 13, continued degradation appears possible beyond the 10^6-cycle "threshold" seen earlier, so it may be more appropriate to think of these thresholds at 10^6 cycles as endurance limits. As figure 13 indicates, there is a large difference in the static interlaminar fracture toughnesses of these materials, shown on the ordinate at N=1, but the cyclic strain energy release rate endurance limits at 10^6 cycles are similar.

Delamination Growth

Although the data in figure 13 shows little difference in delamination durability between brittle and toughened matrix composites, the tough matrix composites will typically exhibit slower delamination growth. Figure 14 shows a

schematic of a log-log plot of delamination growth rate, da/dN, as a function of cyclic strain energy release rates. For the brittle matrix composite, G_c will be low, with an even lower cyclic threshold, G_{th}. Any stable delamination growth under cyclic loading must occur between these two values. Because G_c and G_{th} are very low, delamination growth rates in brittle matrix composites are typically very high compared to crack growth rates in metals. For the toughened matrix composite, G_c will be much higher than for the brittle matrix composite, but G_{th} will be only slightly higher. Because G_c values are much higher than G_{th} values for the toughened matrix composites, slower delamination growth rates are observed. If G_c values are high enough, these growth rates may become comparable to crack growth rates in metals.

FATIGUE ANALYSIS OF COMPOSITE LAMINATES

Composite laminates containing plies of several orientations may experience fatigue failures below their static tensile strength. Figure 15 shows the maximum cyclic load at failure (solid symbols) as a function of fatigue cycles, N, for a $(45/-45/0/90)_s$ graphite epoxy laminate (ref. 12). A fatigue endurance limit was observed around 70 percent of the static tensile strength. The open symbols in figure 15 indicate the onset of 0/90 interface edge delamination, which reaches a plateau around 40 percent of the static tensile strength. Above this threshold, stiffness loss is observed as the edge delamination grows, but fatigue failure does not occur even though the edge delamination may propagate across the width of the laminate. Fatigue failures occur, however, when local delaminations form at matrix ply cracks in the ±45-deg plies. These local delaminations cause isolation of the cracked plies that results in local strain concentrations in the uncracked plies (ref. 14,15). Because of these local

strain concentrations, fatigue failures occur at nominal strain levels below the static failure strain, as illustrated in figure 15 for a quasi-isotropic graphite epoxy laminate.

One technique for estimating the fatigue life of such laminates is being pursued in a joint research program on fatigue of composite materials between the U.S. Army Aerostructures Directorate at NASA Langley and Agusta Helicopter Company under the U.S. Army/ Italian Memorandum of Understanding (MOU). This technique, which is illustrated in figure 16, involves two steps. First, cyclic edge delamination data are used to generate fatigue delamination onset criteria as shown in figures 12,13. This information is then used in the appropriate equations relating applied load to strain energy release rate for local delamination onset to estimate the fatigue failure load as a function of cycles to the onset of local delamination. Under the MOU, this technique will be applied to a variety of composite layups, ranging from orthotropic to quasi-isotropic, for a variety of materials including graphite-epoxy, glass-epoxy, and glass/graphite hybrids.

FATIGUE DESIGN PHILOSOPHY FOR COMPOSITES STRUCTURAL COMPONENTS

Because fatigue failure is a result of the accumulation of delamination sites through the laminate thickness, and because delaminations grow rapidly for most brittle epoxy matrix materials, a no-growth delamination threshold approach for infinite delamination life has been proposed (ref. 12). One concern with this approach in the past has been the uncertainty inherent in predicting service loads which could exceed no-growth thresholds and lead to catastrophic propogation. However, unlike crack growth in metals, catastrophic delamination

growth does not necessarily equate to material or structural failure. Delaminated composites may have inherent redundant load paths that prevent failure and provide a degree of fail safety. This was the case for edge delaminations in the tensile loaded laminates discussed earlier. This degree of fail safety has led designers to think of composite delamination as a relatively benign failure mode. Unfortunately, delaminations may occur from several sources in a given component or structure. Even simple laminates subjected to only cyclic tension loads, experienced an edge delamination first that was relatively benign, followed by local delamination from matrix cracks that caused fatigue failures. Structural components with complex shapes subjected to complex loadings, such as bearingless rotor hubs subjected to combined tension, bending, and torsion loadings, may have a multitude of potential delamination sites. An iterative composite mechanics analysis that considers each of these potential sites must be performed to insure fail safety of the structure. Such an analysis could also be used to identify changes in design details that inhibit delamination. Delamination suppression techniques such as replacement of brittle matrices with toughened matrices, use of adhesive strips in critical interfaces, use of through-the-thickness stitching, and wrapping of the laminate with a reinforced cloth have all suppressed delamination in composites under static loads, but have not been as successful under cyclic loads. Hence, the need for a delamination threshold/fail safety analysis as proposed in ref. 12 is still evident.

CONCLUDING REMARKS

Fracture mechanics has been found to be a useful tool for understanding and characterizing composite delamination. Analyses for calculating the strain

energy release rate associated with delamination growth have been developed for several commmon delamination sources. The strain energy release rate has been found to be a useful generic parameter, independent of layup, thickness, or delamination source, for characterizing delamination failure. ASTM test standards for interlaminar fracture toughness are being developed and have already been used to generate delamination failure criteria. A technique for quantifying delamination durability due to cyclic loading has been developed and is being used to predict fatigue life of composite laminates and to develop a fatigue design philosophy for composite structural components.

REFERENCES

1. O'Brien, T.K.,"Interlaminar Fracture of Composites", NASA TM-85768, 1984, (Also in J. of the Aeronautical Society of India, Vol. 37, No.1, Part III, 1985, p.61.)

2. O'Brien,T.K., "Characterization of delamination onset and growth in a Composite Laminate," in Damage in Composite Materials, ASTM STP 775, June, 1982, p.140.

3. O'Brien,T.K., Johnston,N.J., Morris,D.H., and Simonds,R.A., "A Simple Test for the Interlaminar Fracture Toughness of Composites," SAMPE Journal, Vol.18, No.4, July/August 1982, p.8.

4. O'Brien,T.K., "Mixed-Mode Strain-Energy-Release-Rate Effects on Edge Delamination of Composites," in Effects of Defects in Composite Materials, ASTM STP 836, 1984, p.125.

5. O'Brien,T.K., Johnston,N.J., Morris,D.H., and Simonds,R.A., "Determination of Interlaminar Fracture Toughness and Fracture Mode Dependence of Composites using the Edge Delamination Test," Proceedings of the International Conference on Testing, Evaluation, and Quality Assurance of Composites, University of Surrey, Guildford, England, September, 1983, p.223.

6. O'Brien,T.K., Raju,I.S., and Garber,D.P.,"Residual Thermal and Moisture Influences on the Strain Energy Release Rate Analysis of Edge Delamination," Journal of Composites Technology and Research, Vol.8, No.2, Summer, 1986, p.37.

7. Crossman, F.W., Warren, W.T., Wang, A.S.D., and Law, G.E., "Initiation and Growth of Transverse Cracks and Edge Delamination in Composite Laminates", J. of Composite Materials, Supplemental Volume (1980), pp. 88-106.

8. O'Brien,T.K.,"Fatigue Delamination Behavior of PEEK Thermoplastic Composite Laminates," Proceedings of the American Society for Composites (ASC) First Conference on Composite Materials, Dayton, Ohio, October, 1986., pp. 404-420.

9. O'Brien, T.K., and Raju, I.S., "Strain Energy Release Rate Analysis of Delamination Around an Open Hole in Composite Laminates," AIAA-84-0961, Proceedings of the 25th AIAA/ASME/ASCE/AHS Structures, Structural Dynamics, and Materials Conference, Palm Springs, Ca., 1984, p.526.

10. O'Brien, T.K., "Delamination of Tapered Composite Laminates Containing Internal Ply Drops," to be presented at the 28th AIAA/ASME/ASCE/AHS Structures, Structural Dynamics,and Materials Conference, Monterey, California, April 6-8, 1987.

11. Johnson,W.S., and Mangalgari,P.D., "Influence of Resin on Interlaminar Fracture," in Toughened Composites, ASTM STP 937, 1987.

12. O'Brien, T.K., "Generic Aspects of Delamination in Fatigue of Composite Materials," J. of the American Helicopter Society, Vol. 32, No. 1, January, 1987.

13. Adams,D.F., Zimmerman,R.S., and Odem,E.M., "Determining Frequency and Load Ratio Effects on the Edge Delamination Test in Graphite Epoxy Composites," in Toughened Composites, ASTM STP 937, 1987.

14. O'Brien,T.K., "The Effect of Delamination on the Tensile Strength of Unnotched, Quasi-isotropic, Graphite/Epoxy Laminates," in Proceedings of the SESA/JSME 1982 Joint Conference on Experimental Mechanics, Hawaii, Part I, Society for Experimental Stress Analysis, Brookfield, Conn., May, 1982,p.236.

15. Ryder,J.T., and Crossman,F.W., "A Study of Stiffness, Strength, and Fatigue Life Relationships for Composite Laminates," NASA CR-172211, October, 1983.

SOURCES OF OUT-OF-PLANE LOADS FROM LOAD PATH DISCONTINUITIES

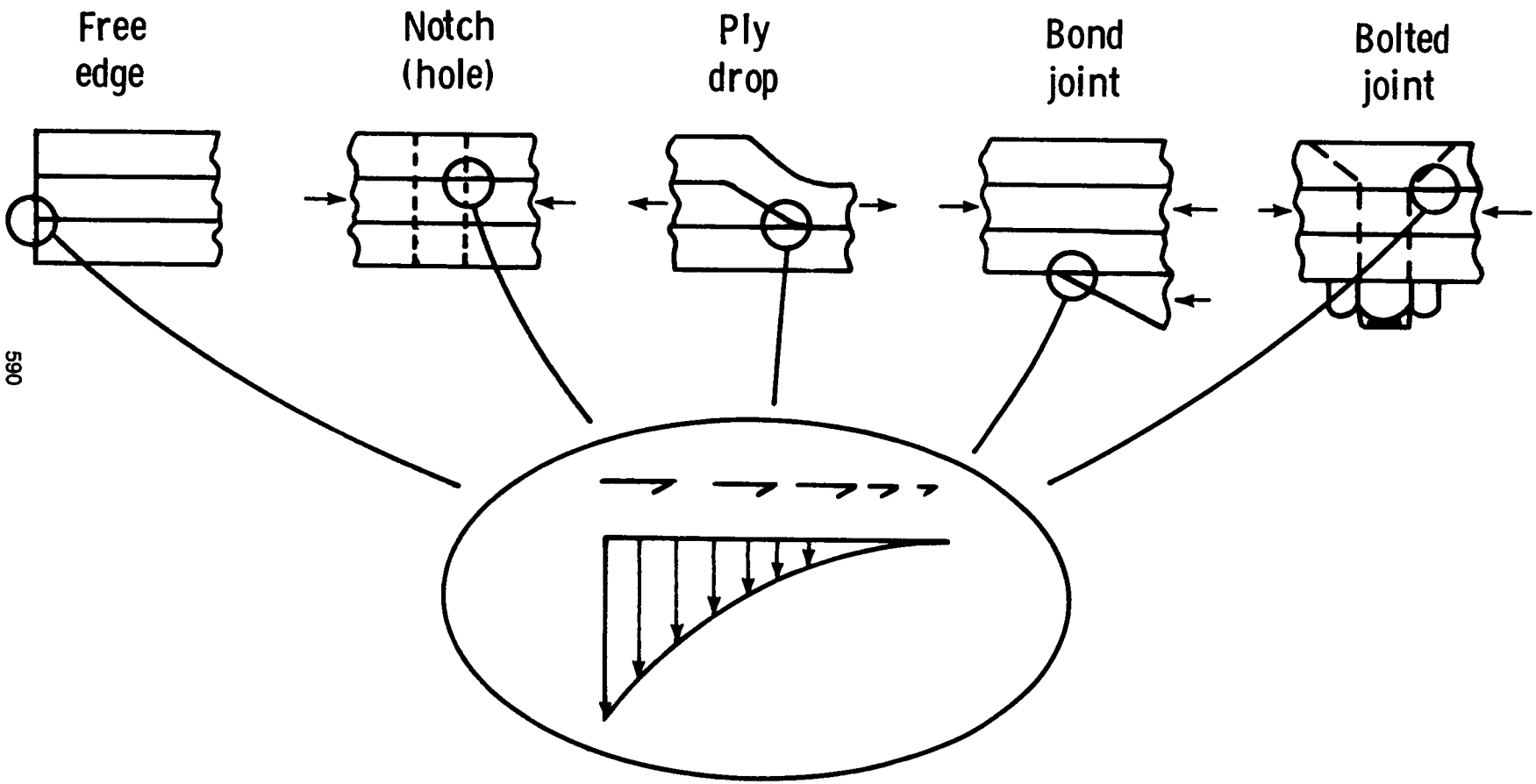

Figure 1.

STRAIN ENERGY RELEASE RATE FOR DELAMINATION GROWTH

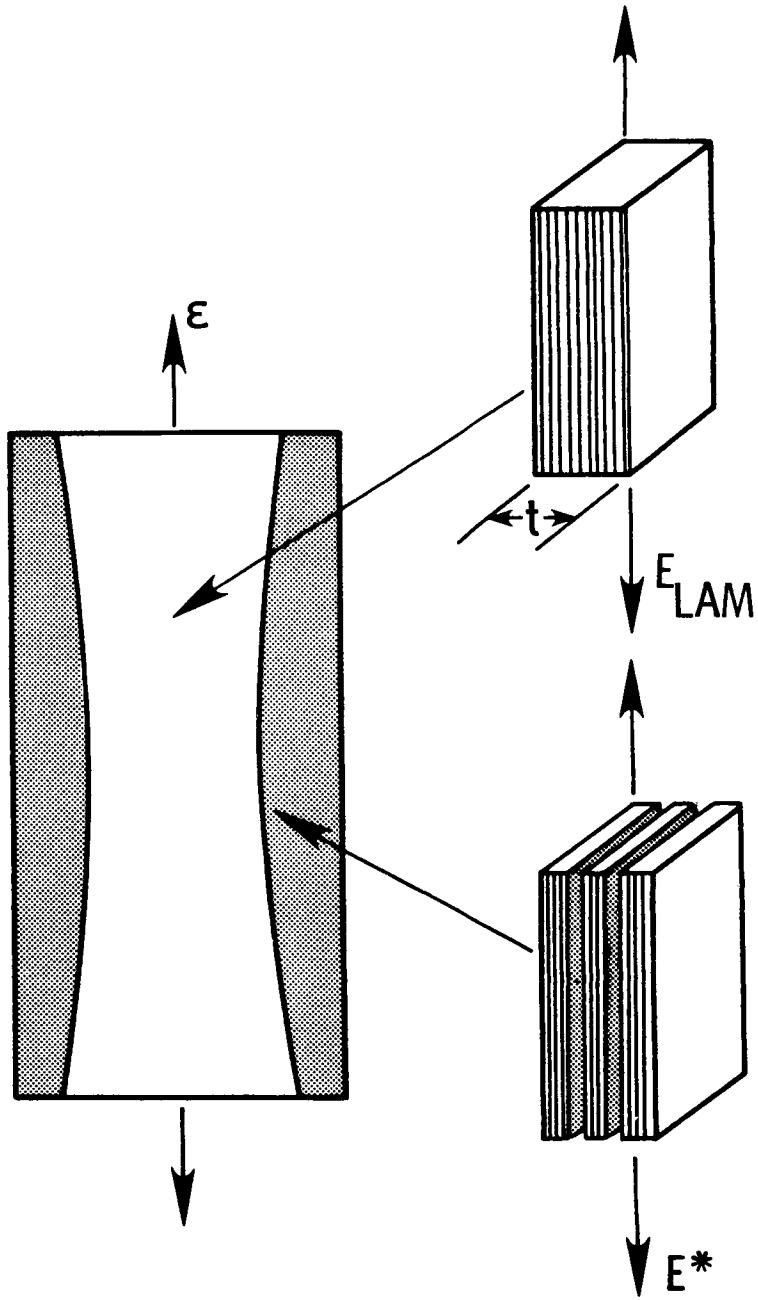

G = strain energy release rate

$$G = \frac{\varepsilon^2 t}{2}\left[E_{LAM} - E^*\right]$$

Figure 2.

DELAMINATION ONSET PREDICTION

Graphite epoxy

$[\pm 45_n/0_n/90_n]_s$

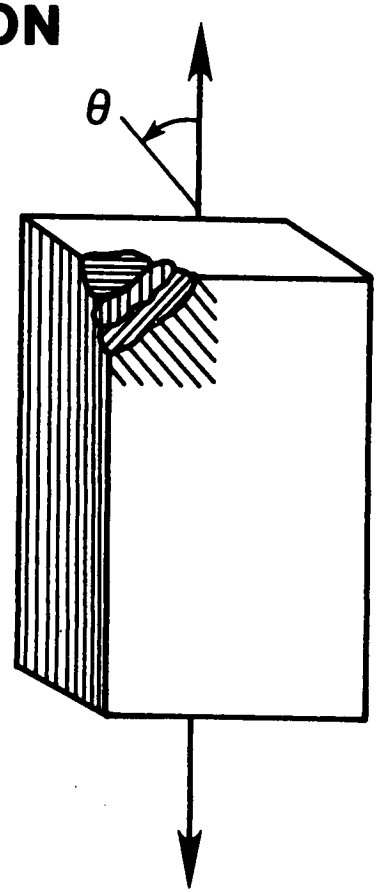

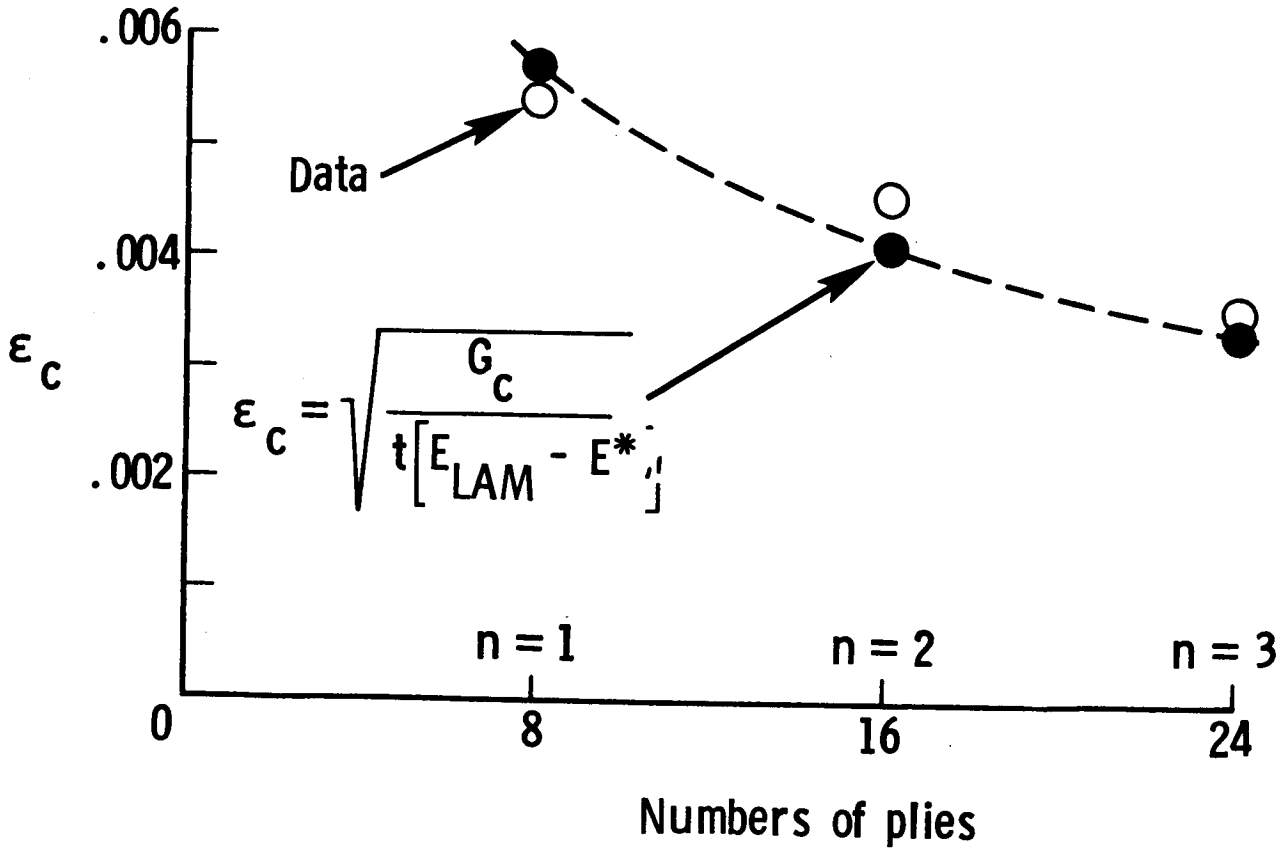

Figure 3

FINITE ELEMENT ANALYSIS OF STRAIN ENERGY RELEASE RATES

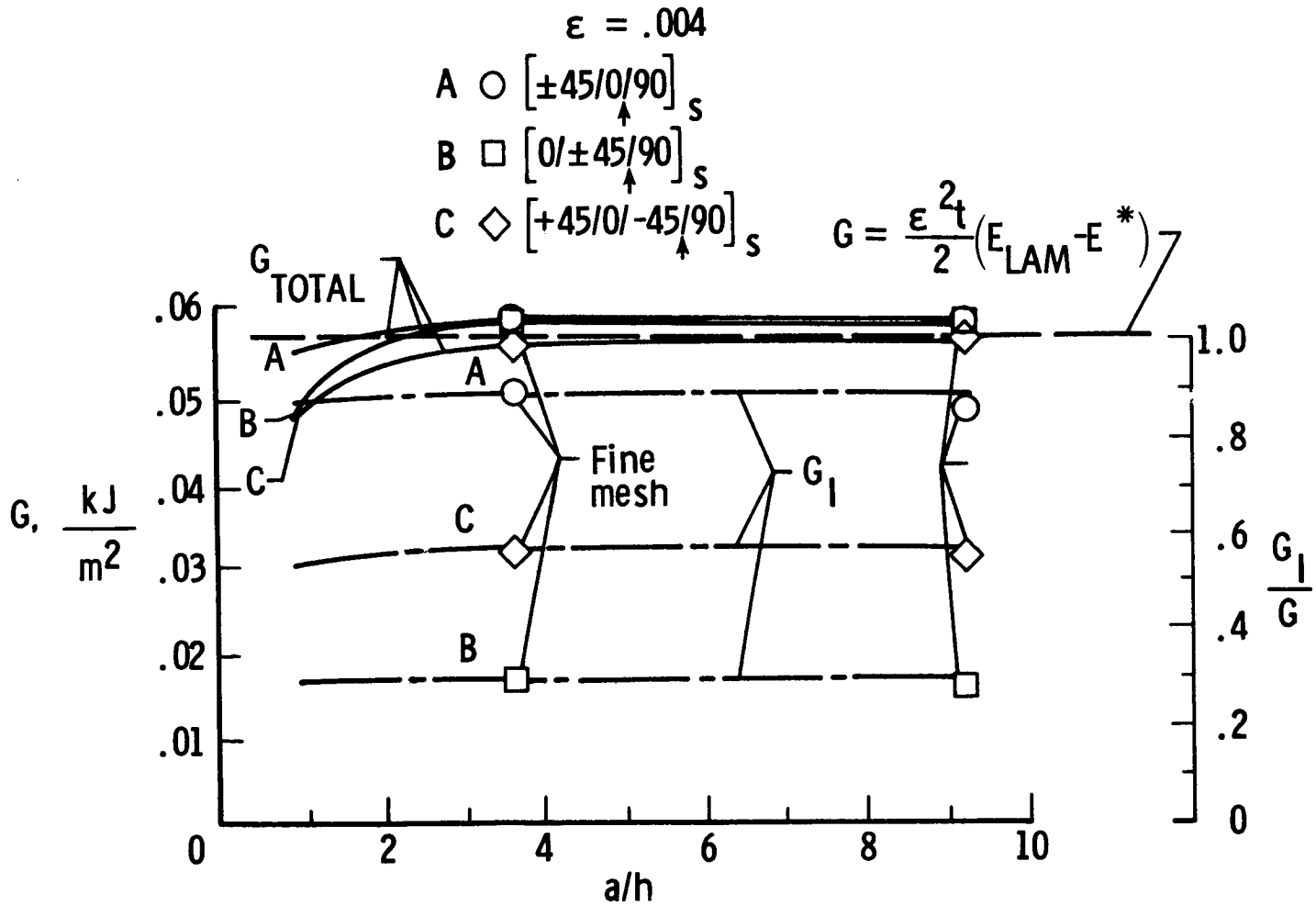

Figure 4.

INFLUENCE OF RESIDUAL THERMAL STRESS ON G FOR EDGE DELAMINATION

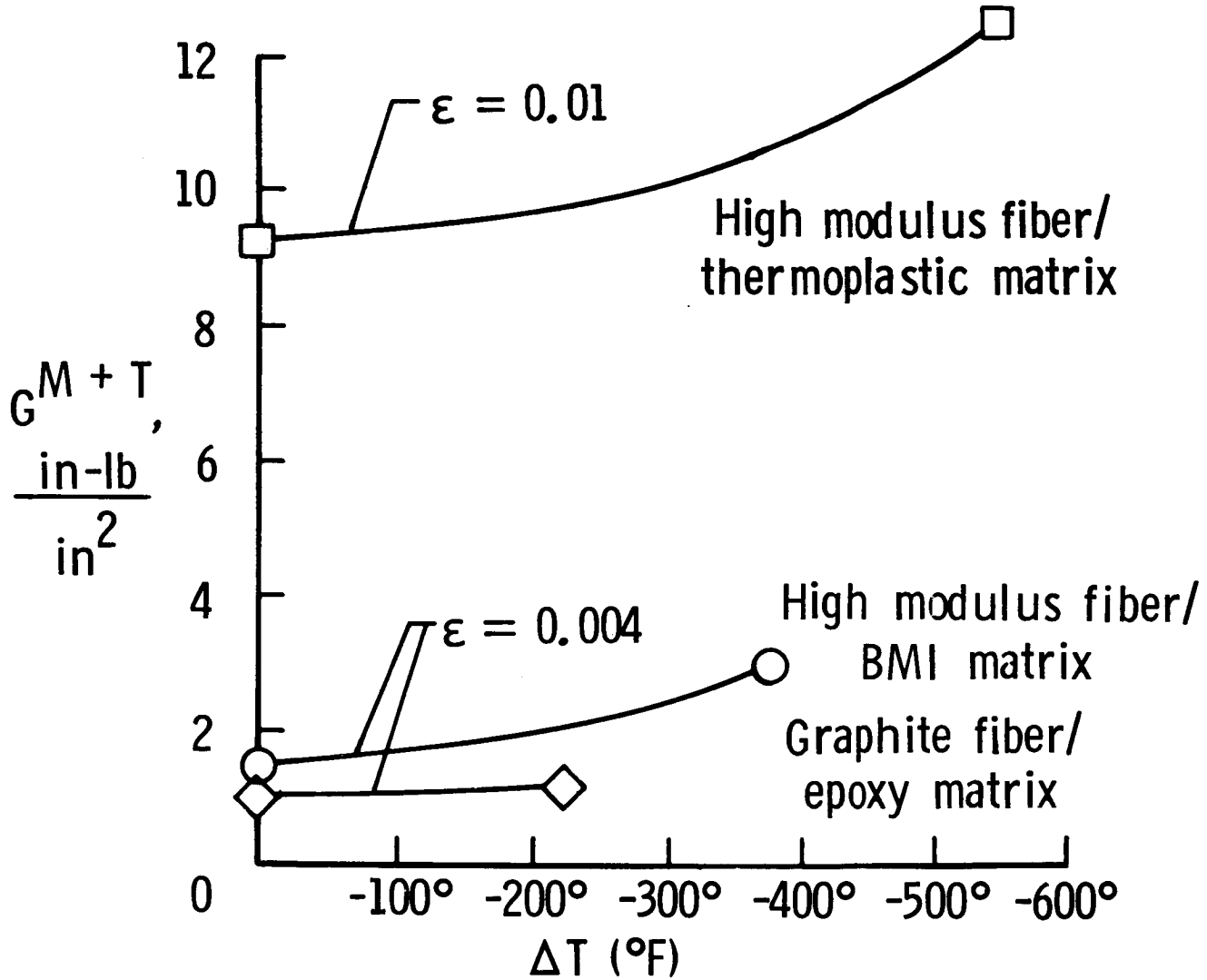

Figure 5.

ROTATED STRAIGHT EDGE ANALYSIS OF STRAIN ENERGY RELEASE RATE AROUND AN OPEN HOLE

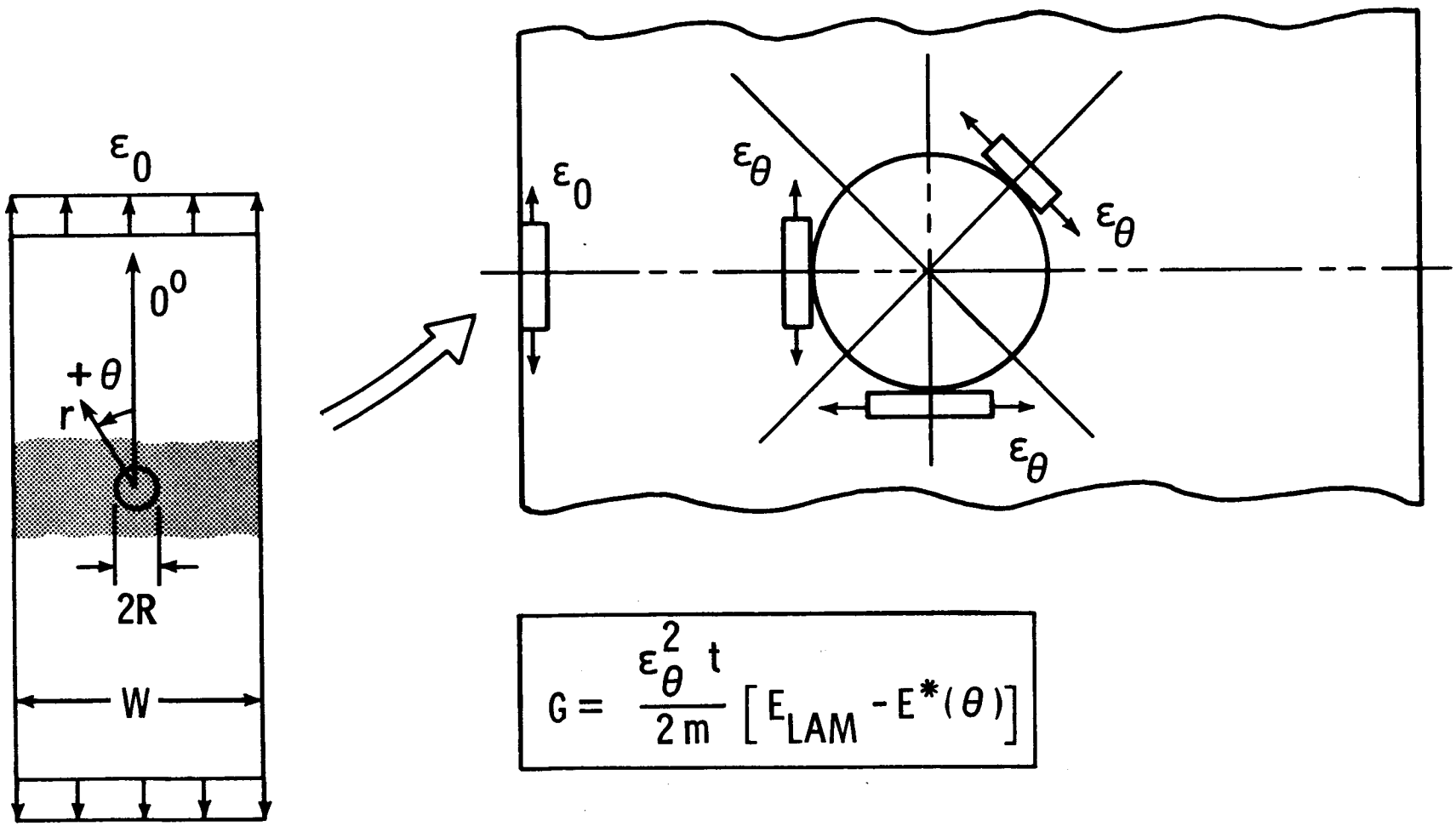

$$G = \frac{\varepsilon_\theta^2 \, t}{2m} \left[E_{LAM} - E^*(\theta) \right]$$

Figure 6.

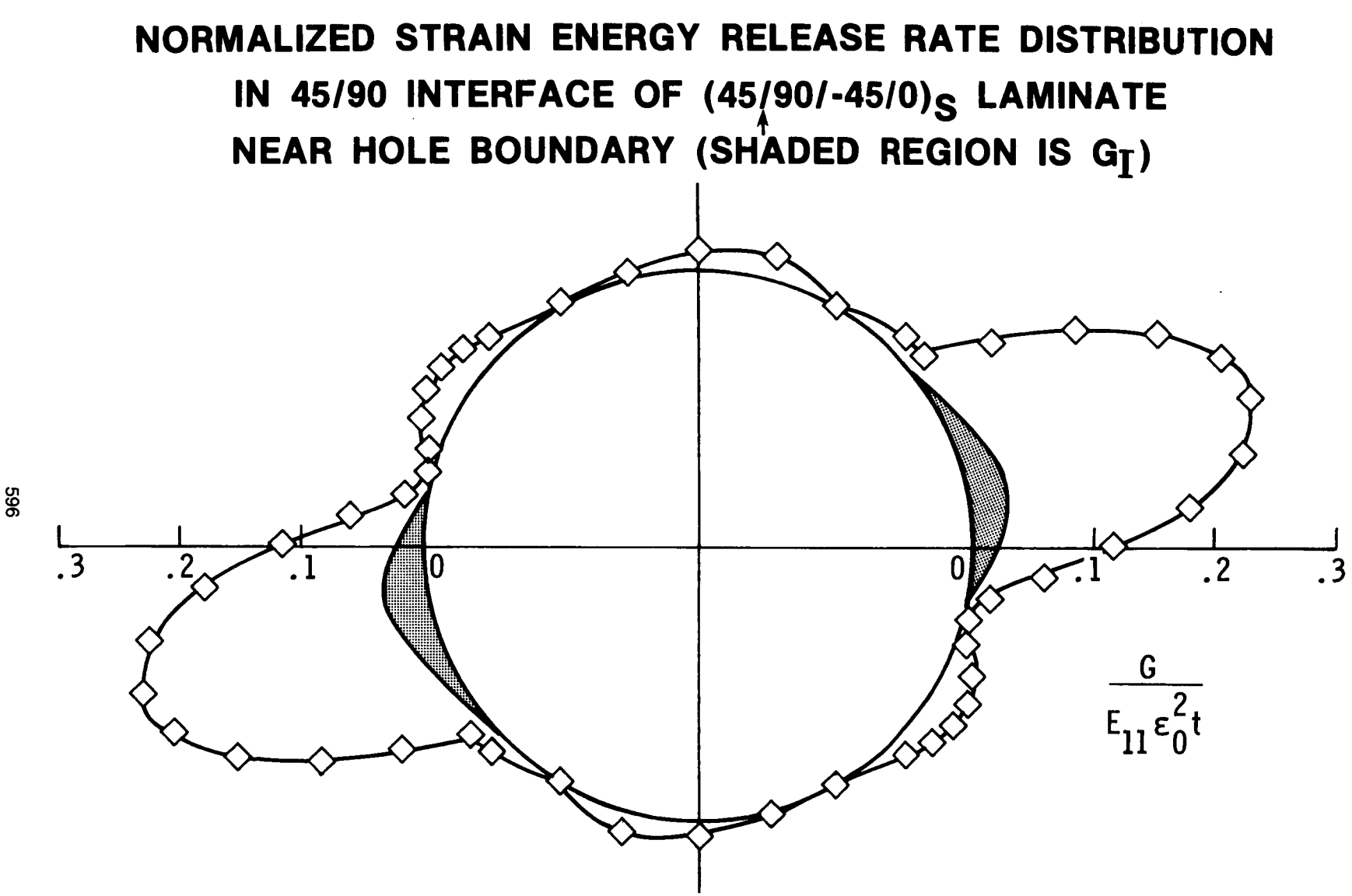
NORMALIZED STRAIN ENERGY RELEASE RATE DISTRIBUTION
IN 45/90 INTERFACE OF (45/90/-45/0)S LAMINATE
NEAR HOLE BOUNDARY (SHADED REGION IS GI)
.3
.2
.1
0
0
.1
.2
.3
G / E11 ε0^2 t
596

Figure 7.

COMPARISON OF DELAMINATION ANALYSES FOR STRAIN ENERGY RELEASE RATE COMPONENTS

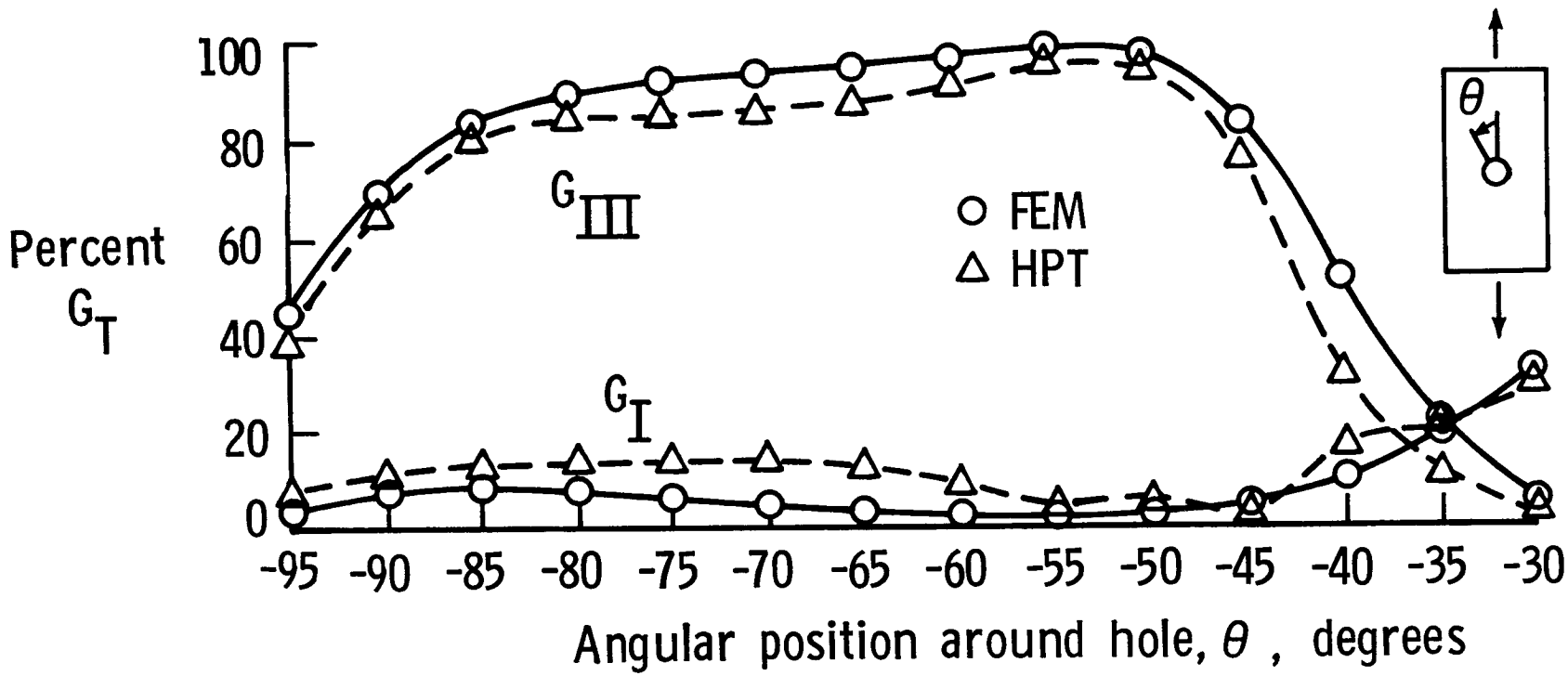

Figure 8.

STRAIN ENERGY RELEASED RATE ANALYSIS OF DELAMINATION IN A TAPERED LAMINATE

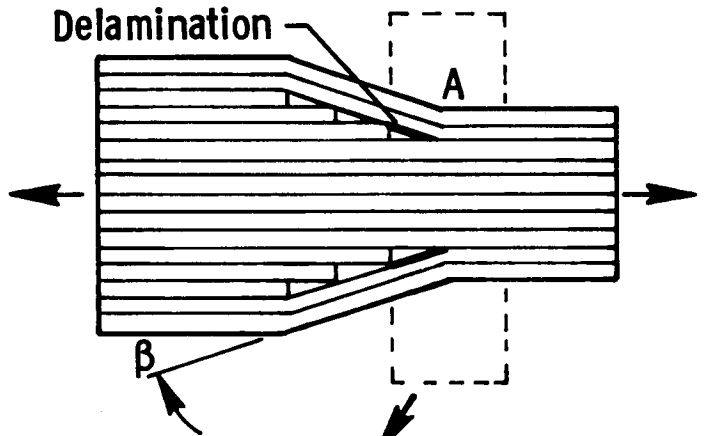

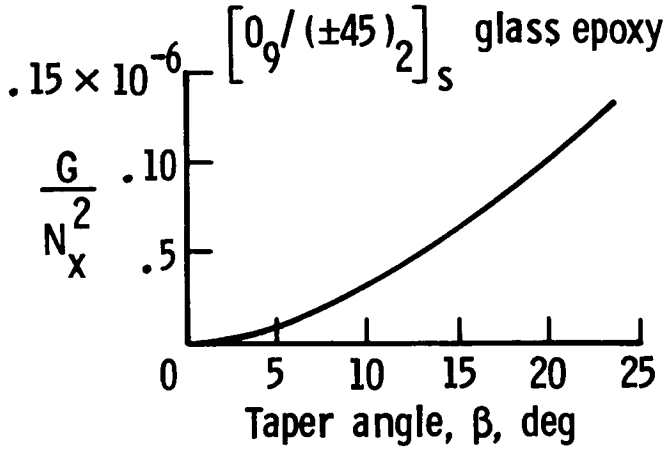

$$G = \frac{N_x^2}{4t}\left(\frac{1}{E^*} - \frac{1}{E_{LAM}}\right)$$

$$E^* = \frac{E_2\ t_2 + E_{core}\ t_{core}}{t}$$

Figure 9.

ASTM ROUND ROBIN
INTERLAMINAR FRACTURE TOUGHNESS TESTING

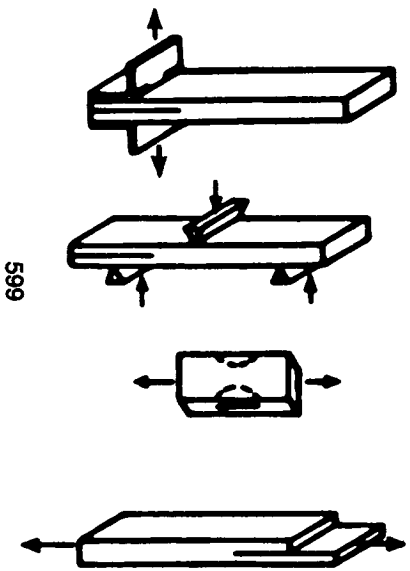

S99

Brittle ⟷ Tough

Test \ Material	AS4/3501-6	AS4/BP907	AS4/PEEK
DCB - Mode I			
ENF - Mode II			
EDT - Mode I and mixed mode			
CLS - Mixed mode			

- 32 laboritories included
- 5 countries represented
- Each participant limited to two tests
- Between 9 and 16 participants per test

Figure 10.

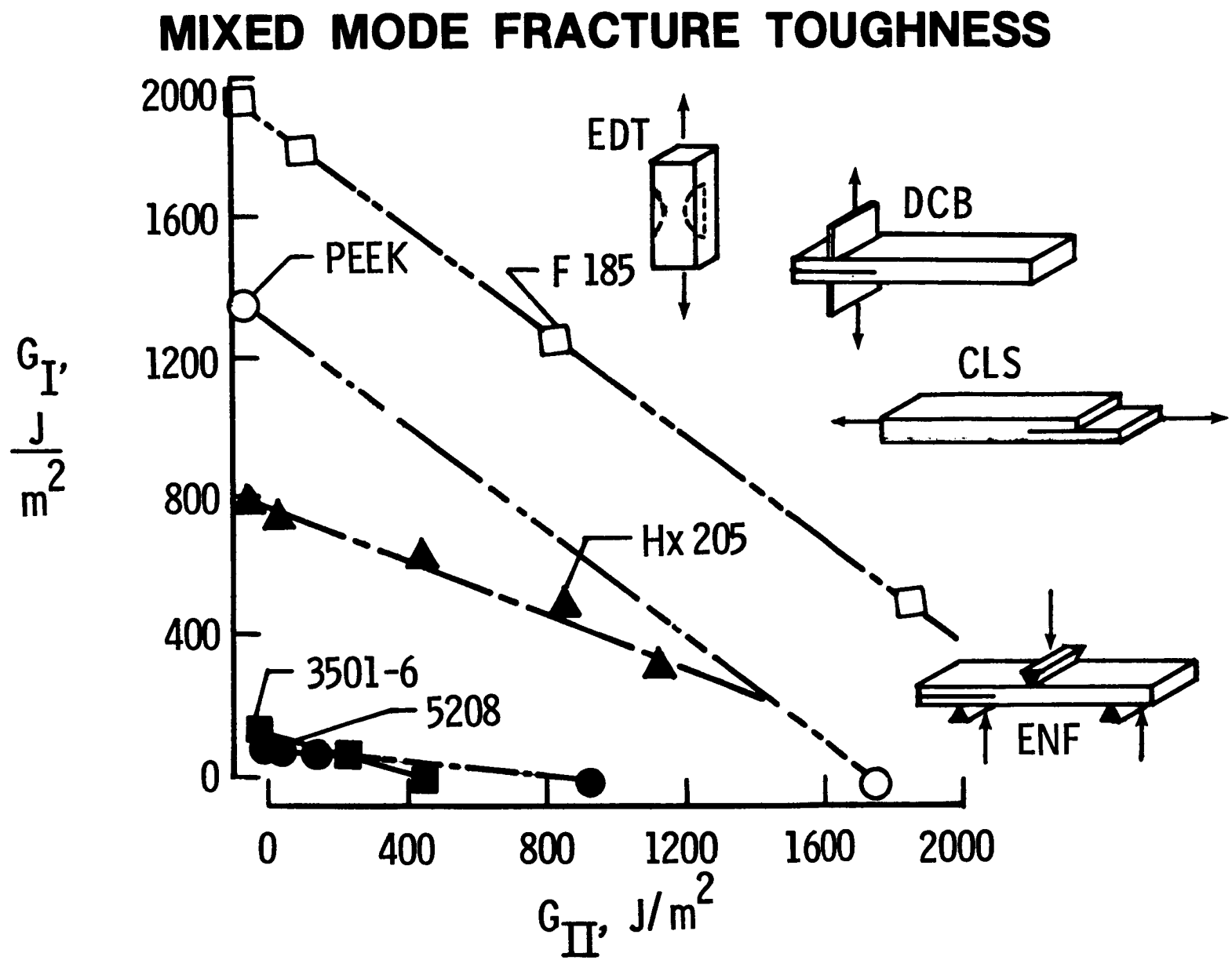
MIXED MODE FRACTURE TOUGHNESS
2000
1600
1200
800
400
0
G_I, J/m^2
PEEK
F 185
Hx 205
3501-6
5208
EDT
DCB
CLS
ENF
0
400
800
1200
1600
2000
G_{II}, J/m^2

Figure 11.

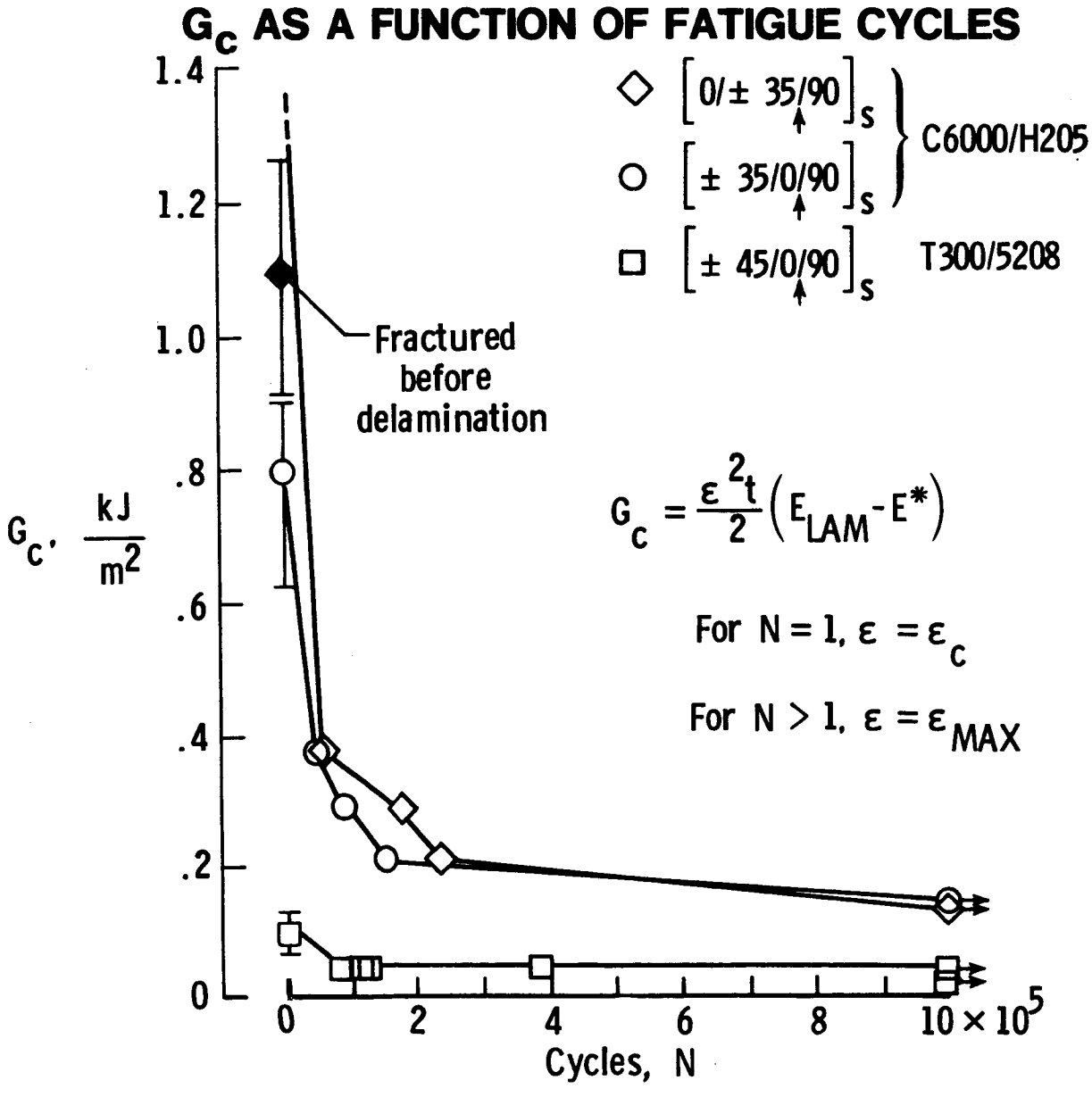
G_c AS A FUNCTION OF FATIGUE CYCLES
◇ [0/± 35/90]s
○ [± 35/0/90]s
C6000/H205
□ [± 45/0/90]s
T300/5208
Fractured before delamination
$G_c = \frac{\varepsilon^2 t}{2}(E_{LAM} - E^*)$
For N = 1, ε = ε_c
For N > 1, ε = ε_{MAX}
G_c, kJ/m²
1.4
1.2
1.0
.8
.6
.4
.2
0
0
2
4
6
8
10 × 10⁵
Cycles, N

Figure 12.

MECHANICAL STRAIN ENERGY RELEASE RATE AT DELAMINATION ONSET AS A FUNCTION OF FATIGUE CYCLES

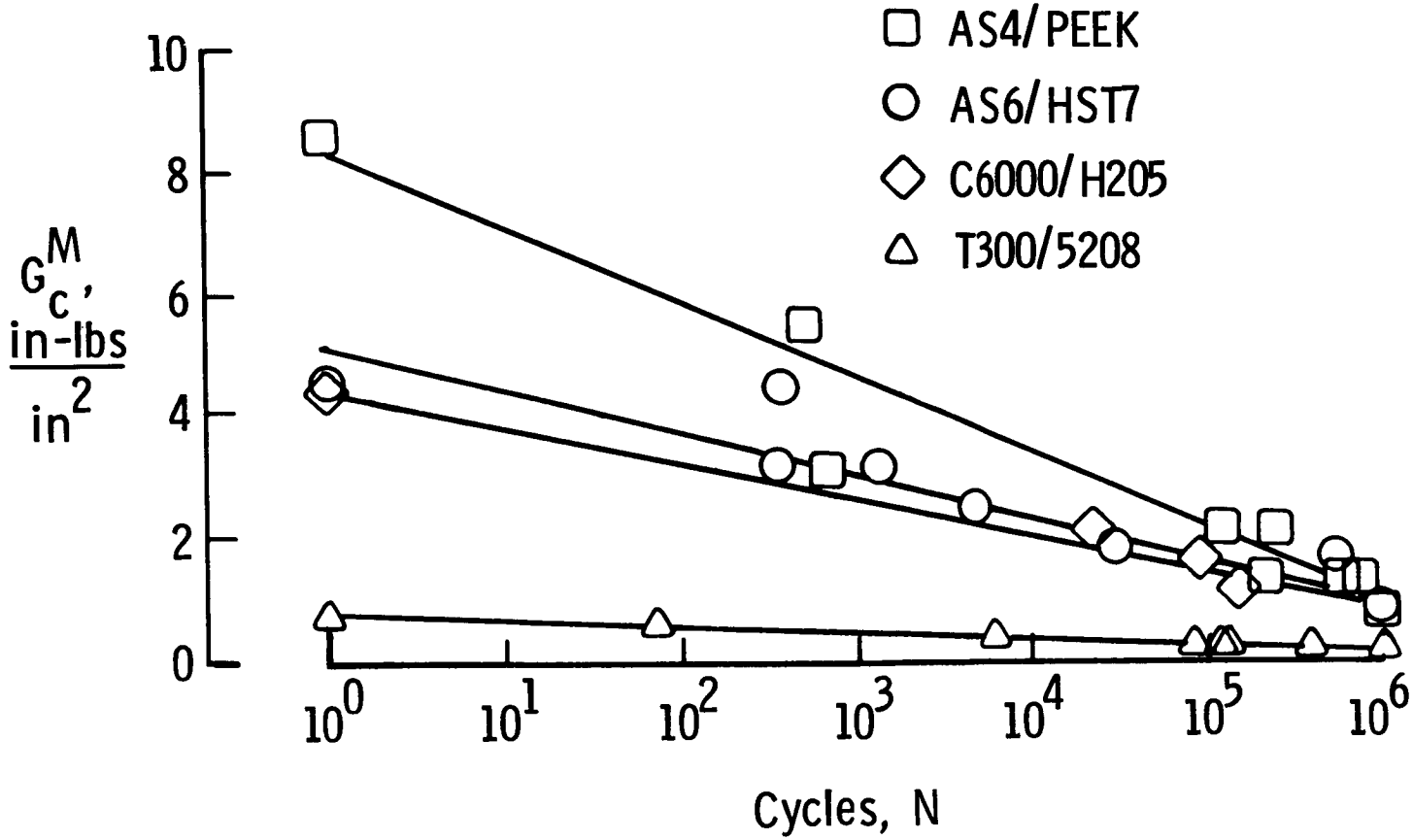

Figure 13.

COMPARISON OF DELAMINATION GROWTH RATES FOR COMPOSITES WITH BRITTLE AND TOUGH MATRICES

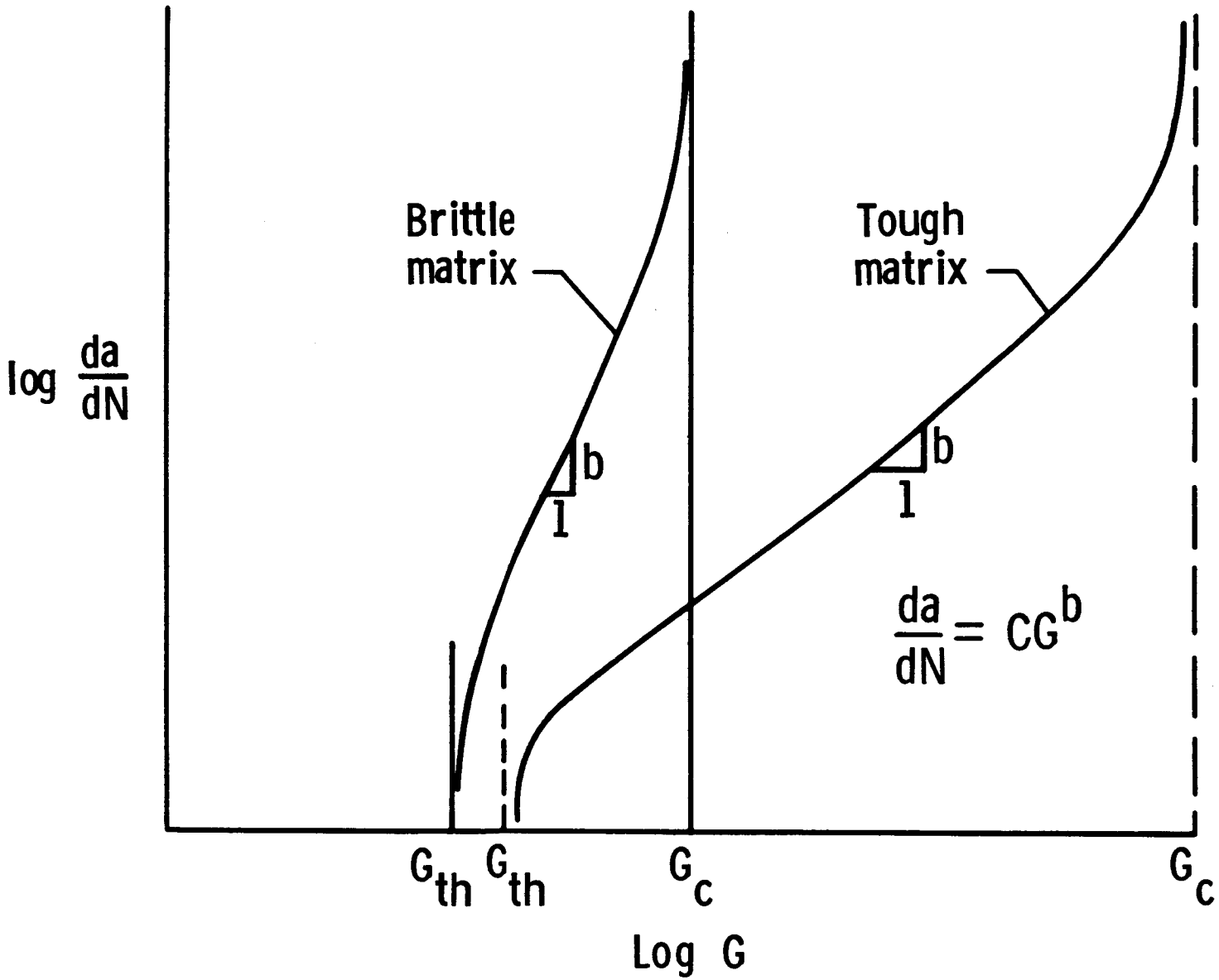

Figure 14.

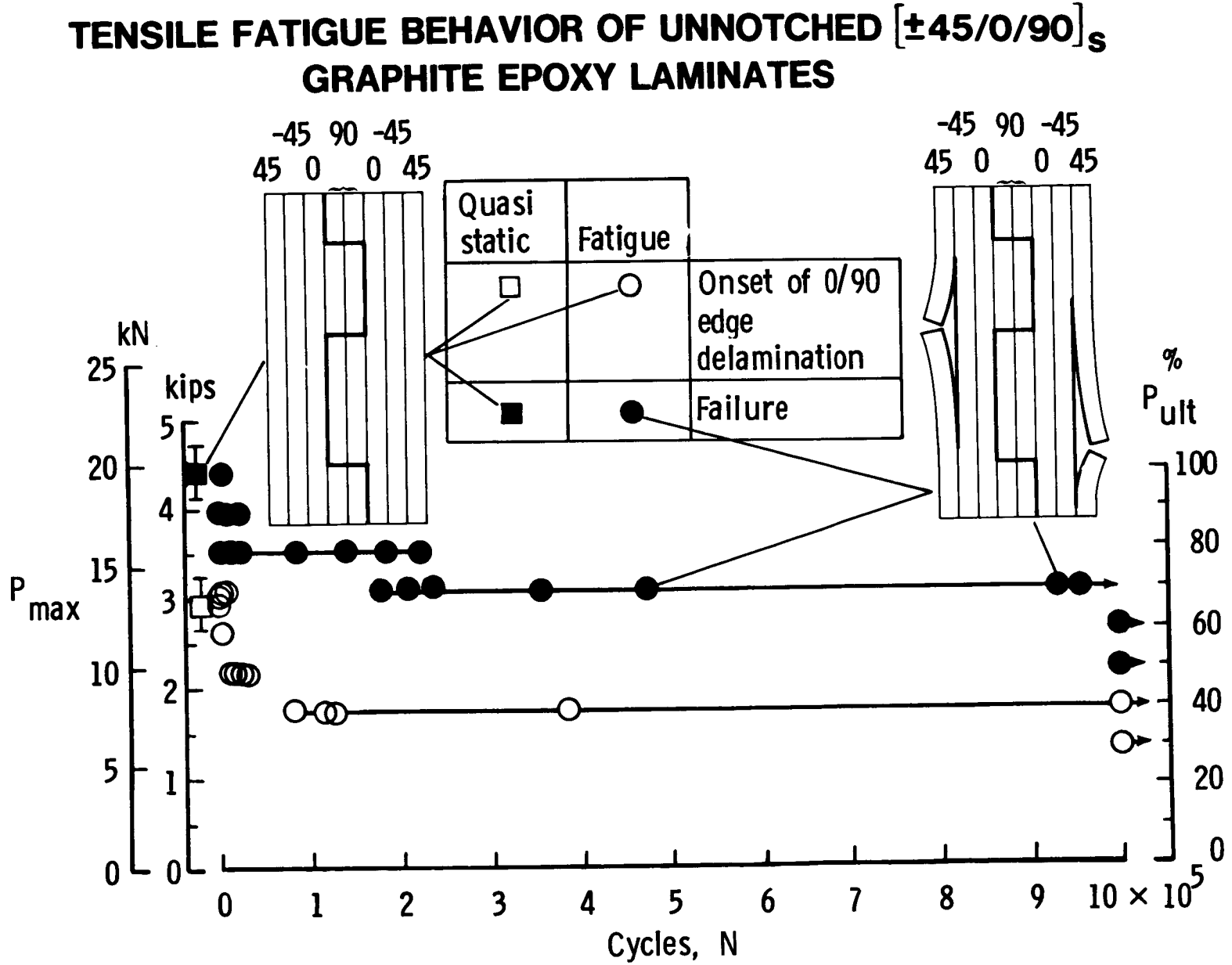
TENSILE FATIGUE BEHAVIOR OF UNNOTCHED [±45/0/90]s
GRAPHITE EPOXY LAMINATES
-45 90 -45
45 0 0 45
Quasi static
Fatigue
Onset of 0/90 edge delamination
Failure
kN
kips
P max
% P ult
Cycles, N
0 1 2 3 4 5 6 7 8 9 10 × 10^5

Figure 15.

FATIGUE LIFE ESTIMATION TECHNIQUE FOR COMPOSITE LAMINATES

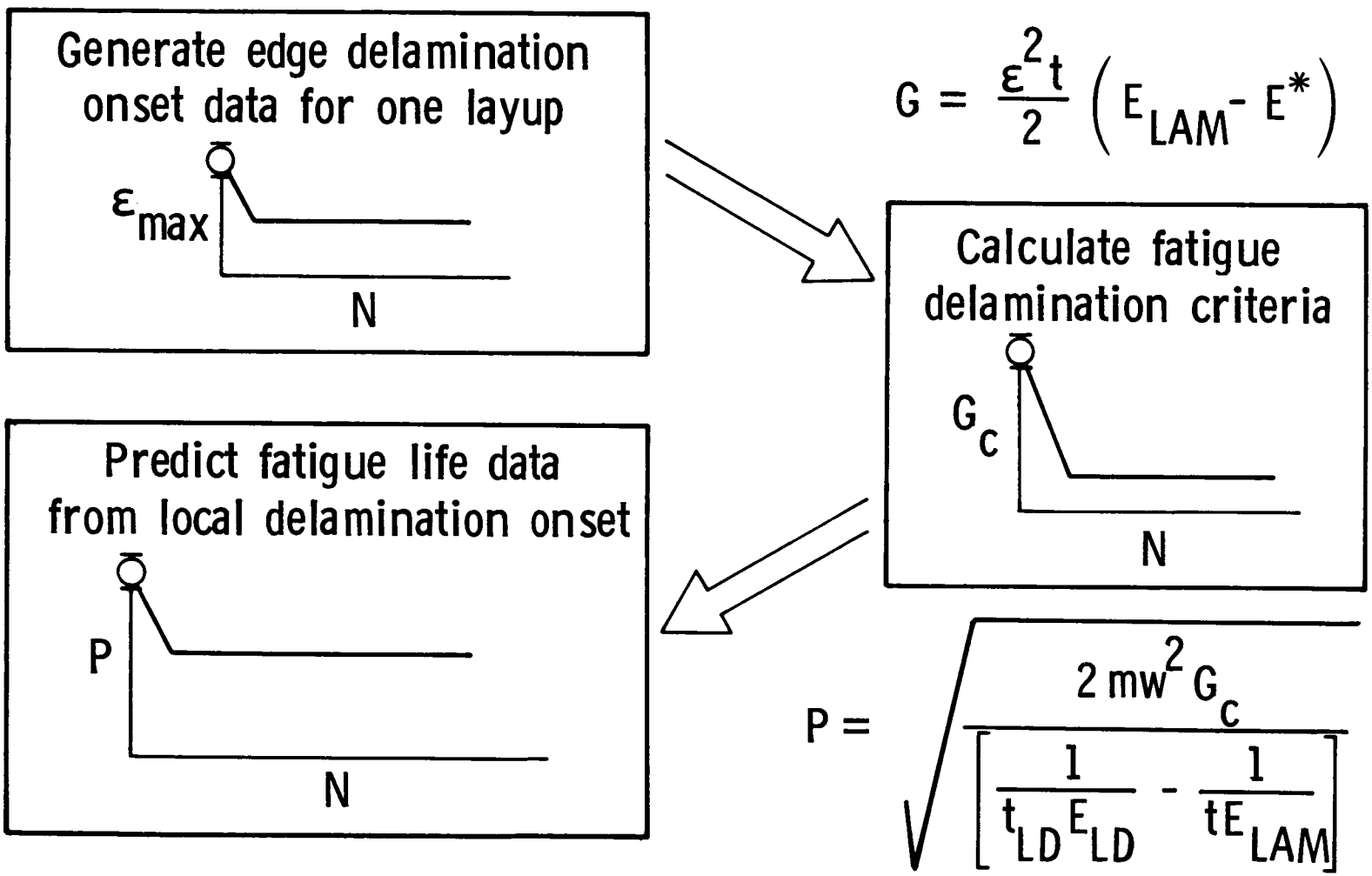

Figure 16.